Checkerboard maps

N. J. Balmforth[a] and E. A. Spiegel
Department of Astronomy, Columbia University, New York, New York 10027

C. Tresser
IBM T. J. Watson Laboratories, Yorktown Heights, New York 10598

(Received 19 January 1994; accepted for publication 11 August 1994)

When a map has one positive Lyapunov exponent, its attractors often look like multidimensional, Cantorial plates of spaghetti. What saves the situation is that there is a deterministic jumping from strand to strand. We propose to approximate such attractors as finite sets of K suitably prescribed curves, each parametrized by an interval. The action of the map on each attractor is then approximated by a map that takes a set of curves into itself, and we graph it on a $K\times K$ checkerboard as a discontinuous one-dimensional map that captures the quantitative dynamics of the original system when K is sufficiently large. © *1995 American Institute of Physics.*

I. THE OPENING

In the description of many natural nonlinear phenomena, one is led to study ordinary differential equations (ODEs) that occur as models, or that govern some relevant part of the dynamics of more complicated evolution equations. The dynamics of an ODE is visualized in its phase space, and the most important features are captured by first return maps on sections through the flow generated by the ODE. Maps also occur directly as models of nonlinear evolution so that understanding the dynamics of maps is central to nonlinear science.

Though great progress has been made in understanding maps from a one-dimensional manifold (an interval or a circle) to itself, maps in higher dimensions are unwieldy and there is no simple way to think about their dynamics, except for special classes of maps. One way to cope with this conceptual difficulty is to capture as much of the original dynamics as possible by a one-dimensional map.

Here we propose some procedures for approximating a higher-dimensional map, f, by a map in one dimension. The procedures we shall describe for doing this are really variations on a single scheme that is effective when there is at most one positive Lyapunov exponent for each orbit. In that case, an attractor of the map typically has the appearance of a collection of finely interwoven strands. Such structures usually involve complicated and fractal geometries, but the dynamics amongst the curves is relatively straightforward; a point lying on one of the curves is mapped into a position on another curve simply according to its location on the original curve.

These observations are the key ingredients in our method, which we may schematize as follows. First we approximate the attractor by a collection of K curves and parametrize each curve by an interval, I_k, with $k=0,1,\ldots,K-1$. Then, using the rules by which points lying along the curves are mapped to other curves, we replace the original map f by a simpler map f_K that takes each I_k into the collection of all intervals. When we regard the I_k as segments of a composite interval, $I(K)$, created by arranging the segments I_k contiguously, we observe that f_K induces a map, $\mathscr{F}_K$, from $I(K)$ to itself. Because the segments are mapped into one another, $\mathscr{F}_K$ is a discontinuous one-dimensional map. It can be visualized by placing pieces of its graph suitably on the grid of rectangles $I_p\times I_q$. Because of the resemblance of this arrangement to the squares of a checkerboard, we call $\mathscr{F}_K$ a *checkerboard map*. The dynamics of $\mathscr{F}_K$ gives a faithful representation of the original dynamics to the extent that the approximation of the attractor by curves is reasonably accurate.

In addition, checkerboarding offers the possibility of producing a one-dimensional map in some cases when the usual procedures for doing this fail. Such cases provide the simplest applications of checkerboarding. Figure 1 shows an example constructed from the Lorenz system

$$\begin{aligned}\dot{x}&=\sigma(y-x),\\ \dot{y}&=rx-y-xz,\\ \dot{z}&=xy-bz,\end{aligned}\tag{1.1}$$

with the parameter value $r=96$. As is usual in constructing a Lorenz map, we have plotted each successive maximum of the variable z as a function of the previous value. In this case, the result is a double-valued function for which the separate curves are easily distinguished and checkerboarded. Figure 2 shows a similar graph for a modified Lorenz system in which the symmetry between the left and right "butterfly wings" is broken by introducing a suitable extra nonlinearity into the equations. The graph of successive maxima in z is again double valued as shown in Fig. 2(b), but it is easily reformulated as the checkerboard of Fig. 2(c). In both examples, given the checkerboards of Figs. 1(c) and 2(c), we know the dynamics of the maxima of z.

In these examples we have simply observed the transition rules between the branches of Figs. 1 and 2, then broken

[a]Present address: Institute for Fusion Studies, University of Texas, Austin, Texas 78712.

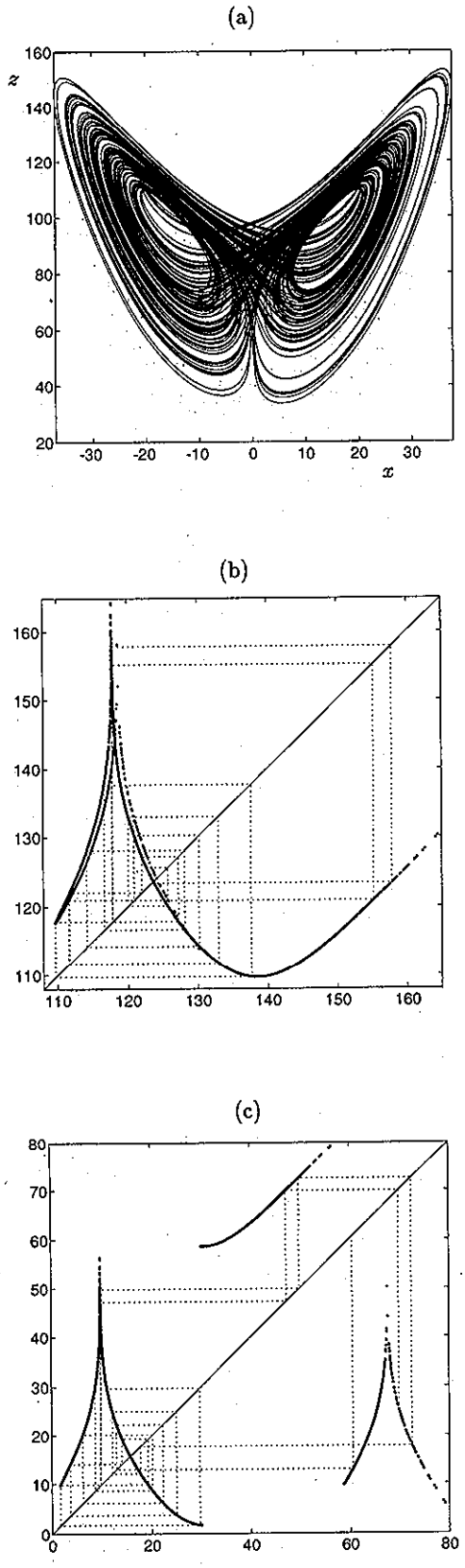

FIG. 1. The Lorenz system at $r=96$, $\sigma=10$ and $b=8/3$. Panel (a) shows a phase portrait projected onto the x-z plane. Panel (b) is a plot of each maximum in z vs its successor. In (c) the pieces of the double-valued function shown in (b) are rearranged into a checkerboard map of an interval. In (b) and (c), a succession of maxima are also drawn.

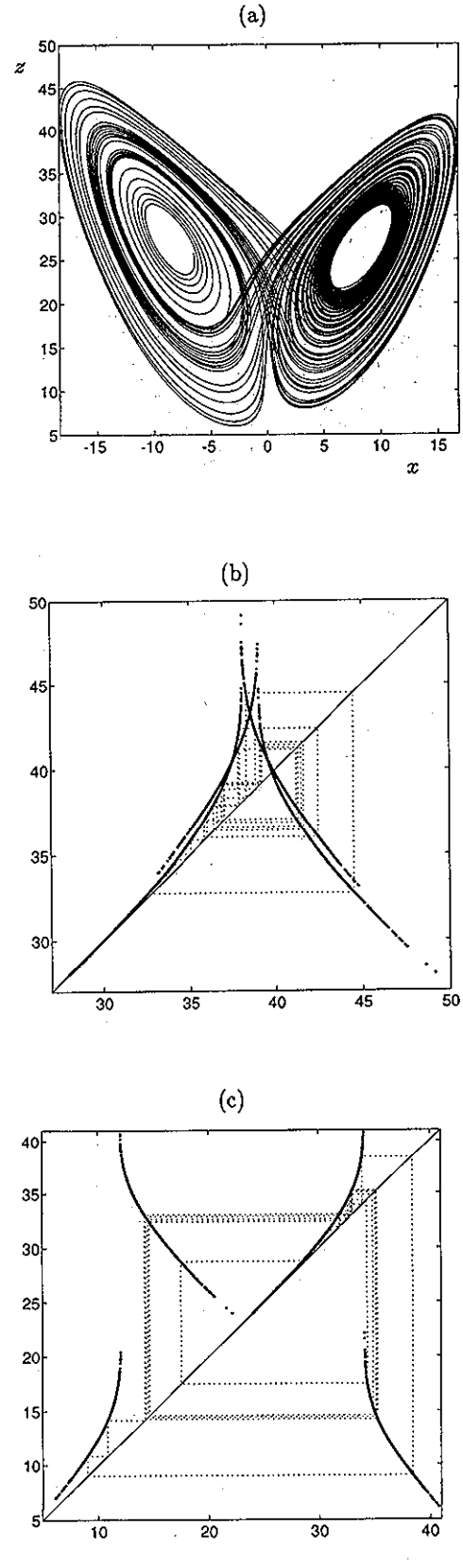

FIG. 2. A modified Lorenz system. Panel (a) shows a phase portrait projected onto the x-z plane. As in Fig. 1(b), panel (b) shows successive maxima in z and this is checkerboarded in (c). This system comprises the Lorenz equations with parameter values $\sigma=10$, $b=8/3$ and $r=28$, plus an extra nonlinear term, $0.05x^2$, in the second equation that breaks the invariance, $(x,y)\rightarrow(-x,-y)$. In (b) and (c), a succession of maxima are also drawn.

up the curves and placed the pieces into a checkerboard accordingly. These examples are based on numerical output computed from a standard chaotic system, but we could as well have constructed illustrations from strings of experimental data. Thus, many cases that do not lead straightforwardly to maps can be made to do so. Maps with attractors that appear to be made up of just a few curves can also be treated in this way.

For systems where we can discern arbitrary numbers of curves in their attractors, such as the Hénon map, the matter is more subtle and we turn to that case next. In the next section, we show two ways to checkerboard the Hénon map. Then, in the third section, we turn to a general statement of our approach and give further illustrations.

II. THE HÉNON GAMBIT

The Hénon map, $\mathbf{H}_{a,b}(x,y)$, which can be written as

$$x'=y,$$
$$y'=1-ay^2+bx, \tag{2.1}$$

takes the plane into itself. Numerical simulations on the Hénon map over a wide range in parameters produce "attractors" that qualitatively resemble collections of curves. As for our opening examples, we could extract a finite number of these curves, break them into pieces and arrange the fragments on a deterministic checkerboard. To proceed in this way we would need to empirically identify and fit the curves. That approach rapidly becomes impractical when we are faced with attractors having Cantorial structure, especially if we want to reach an arbitrary degree of precision. Here we offer two more sophisticated techniques that we can employ to select the curves for the checkerboard.

The first method is based on perturbation theory and uses asymptotic techniques to derive explicit expressions for the curves and the transition rules between them. This method relies on the analytical representation of the map and yields curves that accurately approximate the attractor. The second method is numerically motivated and is adapted to the dynamics of the map rather than its analytical form. Both methods allow us to approximate the Hénon map to arbitrary accuracy with a one-dimensional, discontinuous map. The analytical method contains comparatively fewer curves for a given degree of accuracy, but is more difficult to implement in general than the dynamically founded method.

A. Analytical method

Our asymptotic theory of the Hénon map is motivated by the large dissipation limit ($b\to 0$), in which the map reduces to the quadratic map on the interval. We first rewrite the map (2.1) as

$$y_{i+1}=1-ay_i^2+by_{i-1}. \tag{2.2}$$

When b is small, the final term can be evaluated perturbatively. We rearrange (2.2) into the expression,

$$y_{i-1}=\pm\frac{1}{\sqrt{a}}\sqrt{1-y_i+by_{i-2}}. \tag{2.3}$$

We can iterate this relation to develop high-order approximations for the final term of (2.2). Let

$$Y^1_{i-1-j}=\pm\frac{1}{\sqrt{a}}\sqrt{1-Y^1_{i-j}},\quad j=0,1,\ldots,N-1, \tag{2.4}$$

with $Y^1_i=y_i$. We then construct the quantities,

$$Y^\ell_{i-1-j}=\pm\frac{1}{\sqrt{a}}\sqrt{1-Y^\ell_{i-j}+bY^{\ell-1}_{i-j-2}},$$
$$j=0,1,\ldots,N-\ell,\quad \ell=2,\ldots,N-1, \tag{2.5}$$

and finally

$$Y^N_{i-1}=\pm\frac{1}{\sqrt{a}}\sqrt{1-y_i+bY^{N-1}_{i-2}}. \tag{2.6}$$

This gives an Nth-order approximation to the final term of (2.2). It is computed using y_i and requires the collection of signs appearing in (2.4)–(2.6). If we set $s_{i-j}=\mathrm{sgn}(y_{i-j})$, then we need the *symbol string*, $S_N(i)=(s_{i-1},s_{i-2},\ldots,s_{i-N-1})$, to evaluate the map. Since there are 2^N possible choices for the function, Y^N_{i-1}, we have a one-dimensional map with that many branches.

The symbol string S_N indexes the various curves of the attractor and defines the transition rules, which can be simply represented by $S_N(i+1)=s_iS_{N-1}(i)$. The Cantorial structure of the actual Hénon map is revealed here. As we increase the order of approximation, the number of curves increases like 2^N, and infinite precision is achieved for $N\to\infty$.

Complications in the scheme arise around points for which $y_{i-1}\simeq 0$. There the iteration (2.4)–(2.6) actually diverges and the scheme must be corrected (essentially by inverting the iteration) to restore accuracy. The main repercussion of this problem is that the symbol string, S_N, should no longer be the collection of the signs of y_i. Rather, it is best chosen to be the sign of y_i-y_t, where y_t is the turning point of the current curve of the map.

Checkerboarding can now be formulated as a computational algorithm using the symbol string S_N. We define a number $\mathcal{N}$ written in base 2 as $\theta_{i-1}\theta_{i-2}\theta_{i-3}\ldots\theta_{i-N}$, with $\theta_{i-j}=0$ or 1 if $s_{i-j}=\pm 1$ respectively. Each curve in the asymptotic approximation is labeled by $\mathcal{N}$, an integer lying in the interval $[0,2^N-1]$. If the size of the range in y over which each curve is individually defined is d, then the coor-

dinate on the checkerboard is $X_i = y_i - y_{\min} + \mathcal{N}d$, where $y_{\min}$ is the minimum value of the coordinate y. This variable goes from zero up to $2^N d = Kd$.

Sample checkerboards and their reproductions of the original map are shown in Figs. 3 and 4. In Fig. 3, the checkerboard maps with $N=3$, 4 and 5 are displayed. The pictures show both the map and an illustrative iteration. Checkerboards with larger values of N increasingly resemble parallel dotted lines and their graphs convey little additional information. However, taking the checkerboard modulo one square (by which we mean that the coordinates are taken modulo d) allows recovery of y_i from X_i. The attractors produced in this way approximate that of the Hénon map quite accurately (Fig. 4). Even the relatively simple approximations with 4 and 8 curves contain many characteristic features of the Hénon attractor.

B. Dynamical method

Our second method for deriving the branches of the checkerboard involves considering the dynamics of the map. We assume that the map takes the square $I^2 = [y_{\min}, y_{\min} + d)^2$ into itself. Each vertical line $x = c$ in I^2 is taken by the action of the map into a parabola $\Gamma_c : f(y) = 1 - ay^2 + bc$. Consider the set of parabolas, Γ_α, $\alpha = y_{\min} + kd/K$, with $k = 0,1,\ldots,K-1$. We now construct a $K \times K$ checkerboard composed of elementary squares with sides of length d/K. Segments of the parabolas are the "pieces" that we place on the checkerboard and together they make up the graph of $\mathcal{F}$. Transition rules follow from dividing the plane into strips, $S_{k,K}$, $k = 0,1,\ldots,K-1$ and mapping all points within $S_{k,K}$ onto the parabola Γ_α, with $\alpha = y_{\min} + kd/K$. The strips are given by $S_{k,K} = [y_{\min} + kd/K, y_{\min} + (k+1)d/K) \times [y_{\min}, y_{\min} + d/K)$ and the mapping is effected by projecting the strips $S_{k,K}$ horizontally onto their left boundaries and then applying $\mathbf{H}_{a,b}$. These rules approximate the dynamics of the map. In the limit $K \to \infty$ the strips are infinitely fine and completely foliate the square so that $\mathcal{F}_K$ exactly reproduces the dynamics.

Some checkerboards constructed with this second method are shown in Figs. 5 and 6. In the first picture, checkerboards with 4 and 8 curves are shown. The first panels show the attractors of the checkerboards, modulo one square (which recovers the approximation of the original interval). This checkerboard is manifestly less successful than that of the first method. When we use a large number of curves, however, and work modulo one square of the checkerboard, then we do get a fairly accurate reproduction of Hénon's attractor (Fig. 6).

Surprisingly, when we plot the attractor on the complete checkerboard interval $I(K)$ [Figs. 6(b) and 6(e)], it looks remarkably like the usual Hénon attractor and we understand this as follows. The checkerboard approximation of Hénon's map can be written as

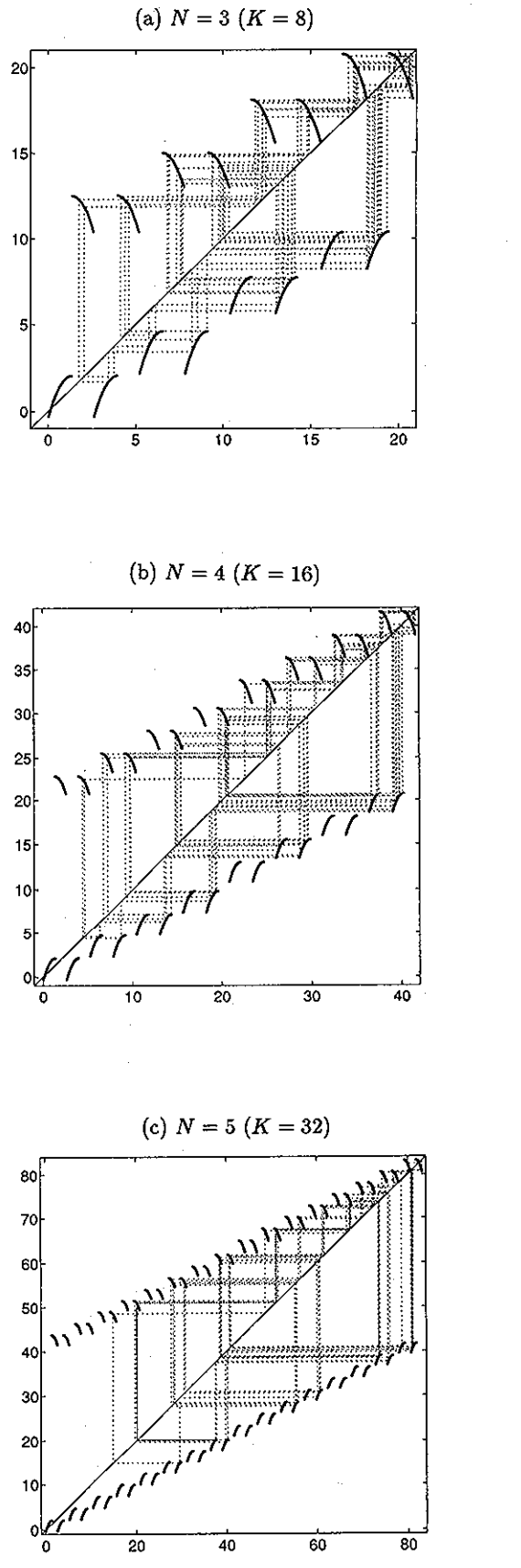

FIG. 3. Checkerboard maps for Hénon's map using the asymptotic method to calculate the curves ($a = 1.4$, $b = 0.3$). The checkerboards for $N = 3$, 4 and 5 (8, 16 and 32 curves) are displayed, together with sample iterations.

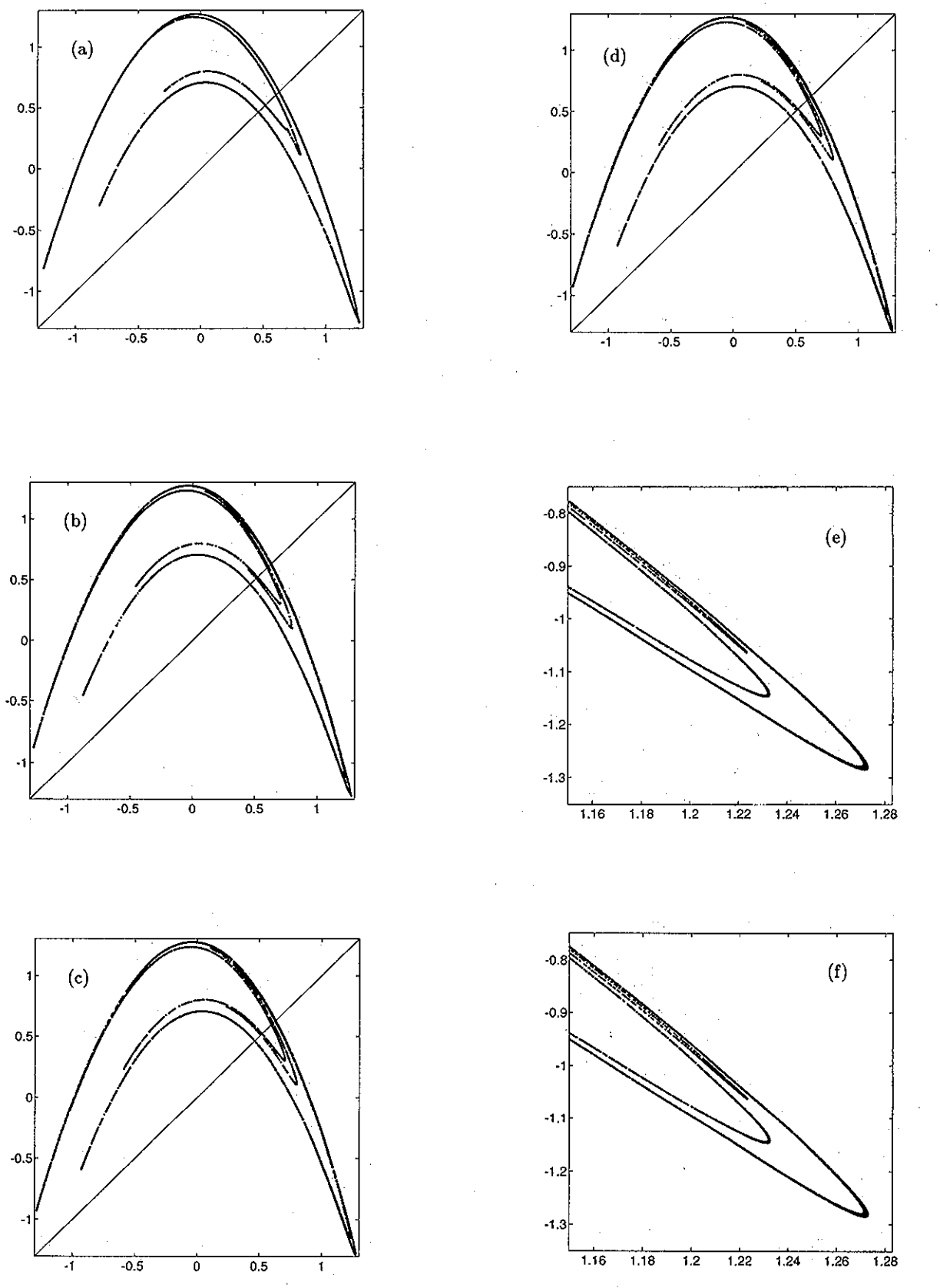

FIG. 4. Reconstructed Hénon attractors using the asymptotic method to calculate the curves. Panels (a), (b) and (c) show the attractor reconstructed with $N=2$, 3 and 10 (4, 8 and 1024 curves) respectively. Drawing the attractors of the approximate map in this fashion amounts to taking the checkerboard modulo one square. Panel (d) shows the actual attractor for comparison, with y plotted against y'. In panels (e) and (f), the rightmost tip of the attractor is shown in more detail for the approximation with $N=10$ and the true map.

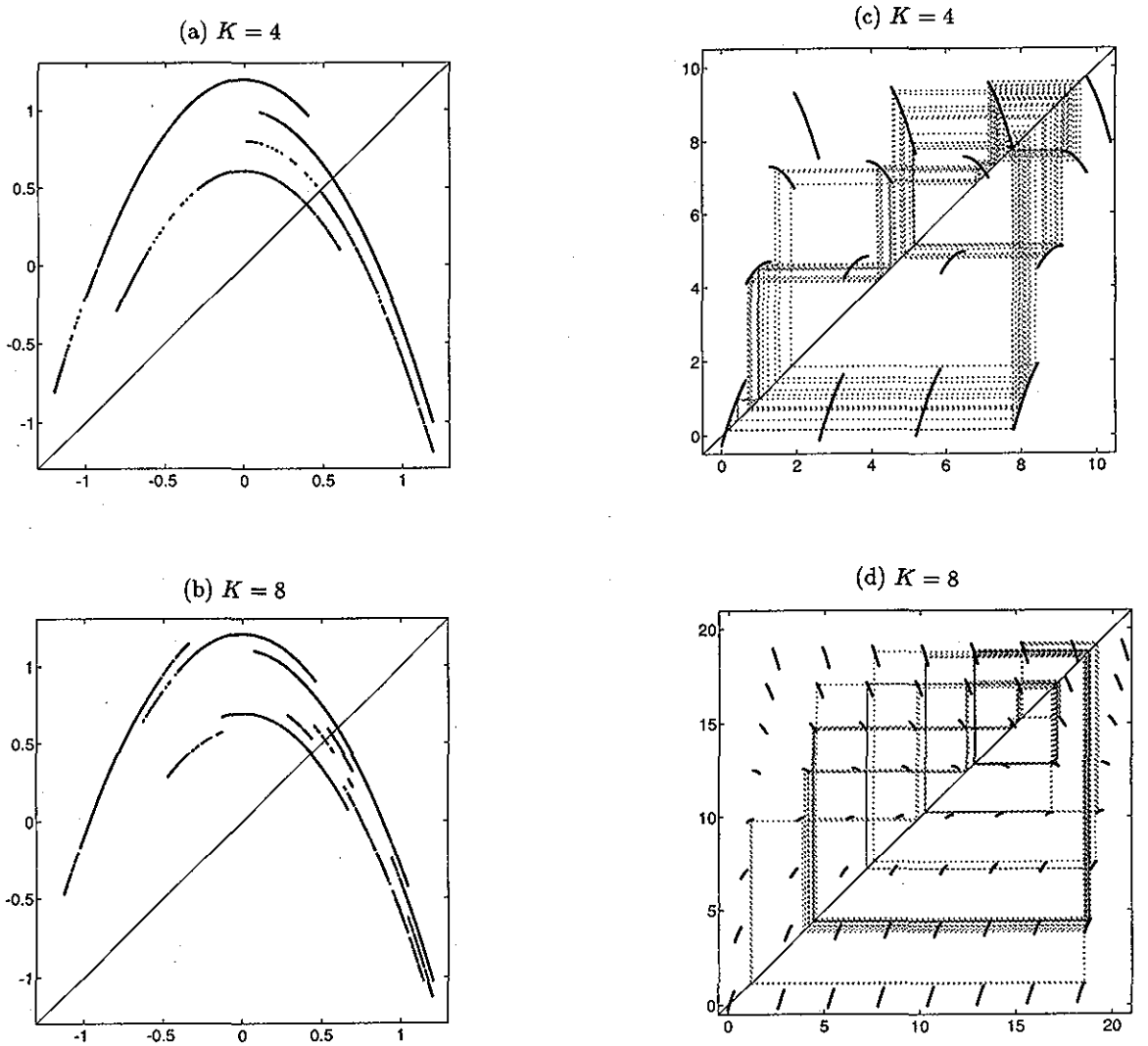

FIG. 5. Checkerboards of the Hénon map using the dynamically founded method. Panels (a) and (c) are constructed with 4 curves; (b) and (d) with 8 curves. In panels (a) and (b), the approximation of the Hénon attractor is shown (y against y'), on taking the checkerboard modulo one square. Panels (c) and (d) display the checkerboard map plus a sample iteration sequence.

$$X' = 1 - a\left(d\left\{\frac{X}{d}\right\} + y_{\min}\right)^2 + b\left(\frac{d}{K}\left[\frac{X}{d}\right] + y_{\min}\right) + y_{\min} + d\left[K\left\{\frac{X}{d}\right\}\right], \tag{2.7}$$

where $\{Z\}$ means fractional part (modulo one), and $[Z]$ means integral part of Z. When K is sufficiently large, a plot of X' against X is dominated by the final term of (2.7). In other words, although the dynamics is controlled by the whole expression, the checkerboard map looks like a plot of $d[K\{X/d\}]$ against it previous value. But $d[K\{X/d\}]$ is approximately $K(y-y_{\min})$, and its previous value was $K(x-y_{\min})$. The picture should therefore be our approximation of the Hénon map, offset and scaled by K. Note that this result is not a universal feature of checkerboarding but is a consequence of the explicit form of the Hénon map. This leads us to discretize the coordinate x, in effect.

The histograms of Fig. 7 contrast the accuracies of numerically computed trajectories for the two checkerboarding schemes for the Hénon map. At the kth step, we have recorded y and its previous value, and computed y' using both the Hénon map and the checkerboards from the two methods just described. We then measured an absolute error at the kth step, and its logarithm, $\mathscr{E}$, is shown in the pictures. The error in the first case depends on the order N. Roughly, we have $\mathscr{E} \sim \log_{10} b^{N+1}$. For the second method, the controlling factor is just the number of curves and $\mathscr{E} \sim 1/K$. In both cases, we can approximate the Hénon map by a one-dimensional checkerboard to single and even double precision.

III. THE ENDGAME

In some sense, what we have been doing is to make explicit what many must sense implicitly. Now we formalize a general procedure for checkerboarding a multidimensional map. To illustrate this, we consider first a map of the square

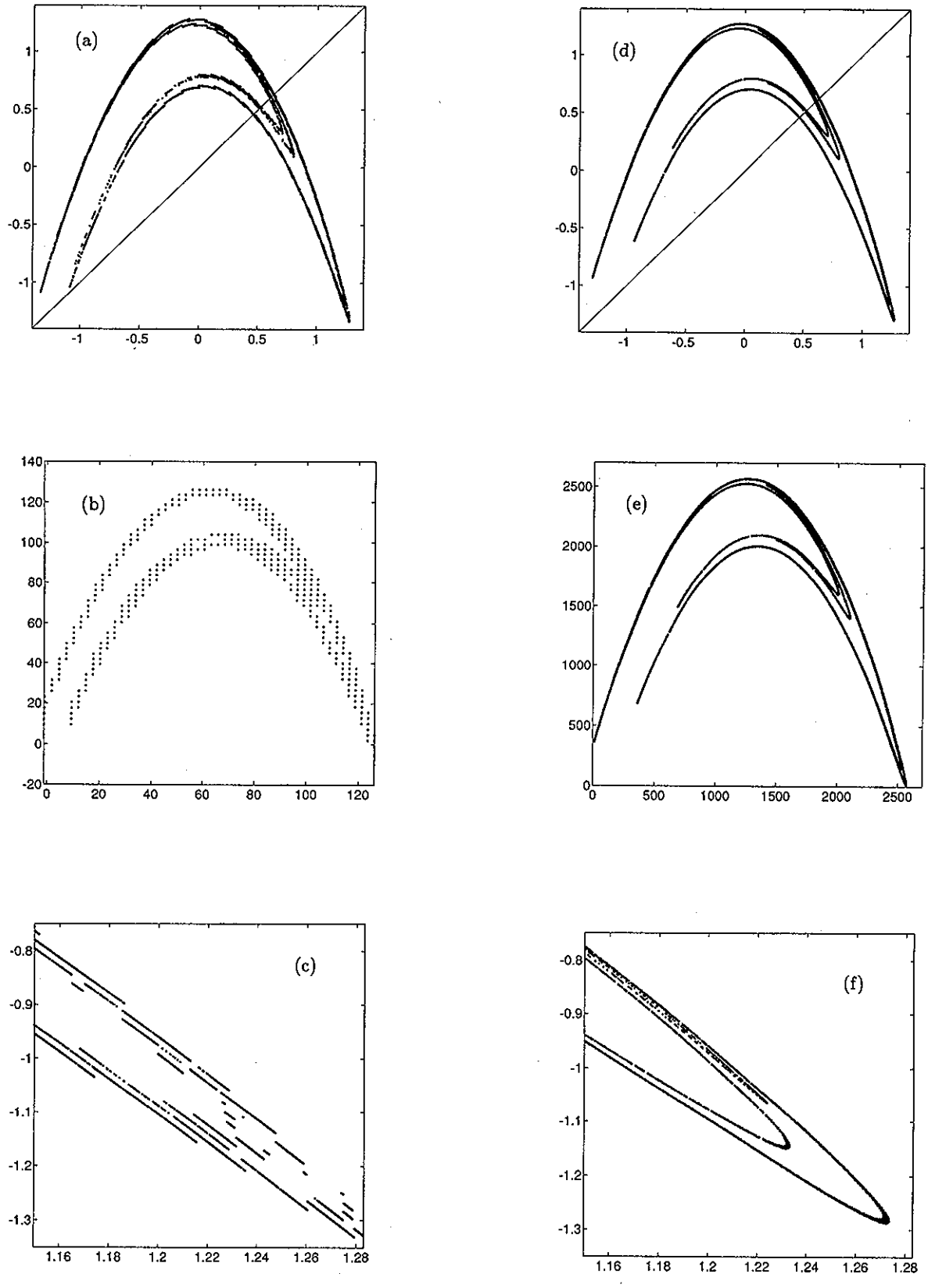

FIG. 6. Checkerboards of the Hénon map using the dynamically founded method. Panels (a)–(c) are computed with 100 curves; panels (d)–(f) with 1000 curves. The attractors, modulo one square of the checkerboard, are shown in (a) and (d). The checkerboards themselves are portrayed in (b) and (e). Panels (c) and (f) show the rightmost tip in more detail.

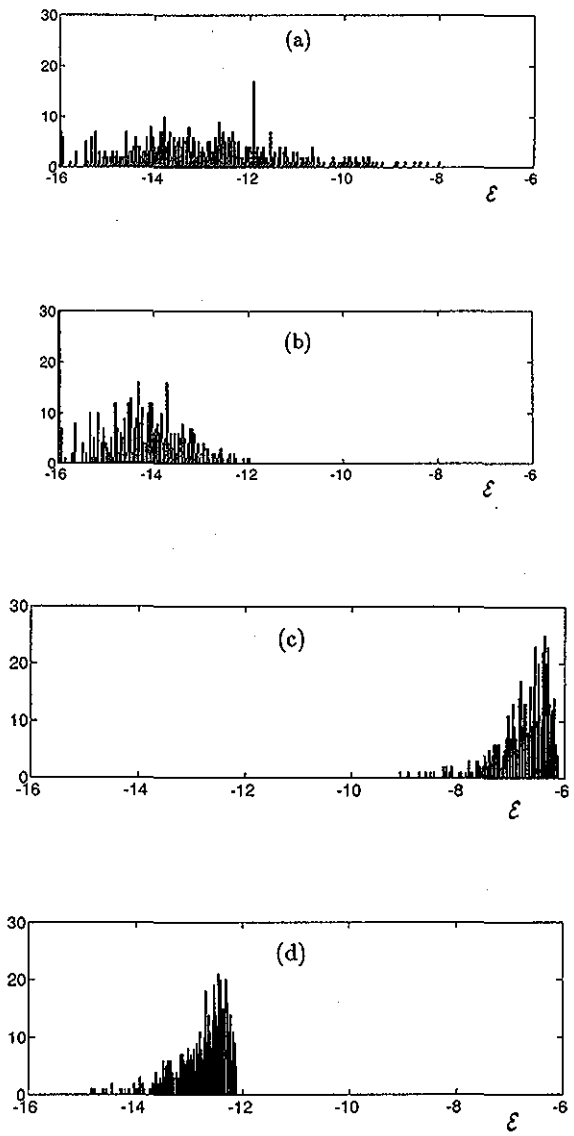

FIG. 7. Histograms of the logarithm of the absolute error, $\mathcal{E}$, for the two checkerboard approximations of the Hénon map. Shown are the errors incurred over a sequence of 500 iterations for checkerboards with different levels of approximation. In panels (a)–(b), error for the first checkerboarding method is shown for approximations with $N=20$ and 40. In (c)–(d), the error in the second method is shown for $K=10^6$ and 10^{12}.

into itself. We endow the square with K parallel intervals, I_k, $k=0,1,\ldots,K-1$, arranged regularly across the square. This cuts the square into strips whose (disjoint) union is the original square. The operation of the original map on the edge of each of the strips generates the pieces to be put into the squares of a checkerboard map.

More generally, consider the hypercube $I^n:=I\times I\times\ldots\times I$ where $I:=[0,1)$. Suppose we are given a map, f, that takes I^n into itself. As with the square, we pierce the hypercube with parallel intervals, I_k, with $k=0,1,\ldots,K-1$ and we regard the hypercube as $I^n=I\times I^{n-1}$, where I is some particular interval parallel to the I_k. The success of the procedure depends on the choice of the distinguished interval, I.

We partition the hypersurface I^{n-1} into scaled copies of itself with edges of length $1/m$, where m is defined so that $K=m^{n-1}$. Now I^{n-1} is the disjoint union of these copies, denoted as P_k. Correspondingly, I^n is the disjoint union of parallelopipeds $\mathscr{P}_k=I\times P_k$. Each parallelopiped $\mathscr{P}_k$ can then be approximated by its unique edge of unit length, I_k.

Now $F_{K,k}$ is the map from I^n to the composite interval $I(K)$ sending $\mathscr{P}_k$ to $I_k\subset I(K)$ by an orthogonal projection. We can approximate the map $f:I^n\to I^n$ by

$$\mathscr{F}_K=F_{K,k}\circ f\circ F_{K,k}. \tag{3.1}$$

This new map takes the interval $I(K)$ into itself.

With this general approximation procedure, we can checkerboard many different kinds of maps, and here we give a few more illustrations. In Fig. 8, we show Shil'nikov's map, defined by

$$\begin{aligned} x' &= 1+bxz^{\delta}\sin(\xi\log z+\phi),\\ z' &= xz^{\delta}\cos(\xi\log z+\phi), \end{aligned} \tag{3.2}$$

with $b=0.15$, $\delta=0.5$, $\xi=3$, and $\phi=1.1837$. Like the Hénon example, we checkerboard this map by covering the plane with strips defined by lines of constant x. This gives the 10^2-curve and 10^3-curve approximations also shown in Fig. 8. As a result of the foliation of the plane by the coordinate x, the attractor of the checkerboard map looks like a plot of x against x' for a sufficiently large number of curves (exactly as in the Hénon example). The attractor modulo one square resembles z against z'.

So far we have been concerned with maps on n-dimensional intervals. However, since we can also regard I as parametrizing a circle, our method is more adaptable and we can checkerboard maps on annuli, tori and, more generally, on the space $\mathbb{T}^p\times I^m$, where $\mathbb{T}^p$ is the p-dimensional torus. As an example, Fig. 9 shows the annulus map,

$$\begin{aligned} \theta' &= \theta+\Omega+\lambda r+\mu\sin\theta,\\ r' &= \lambda r+\mu\sin\theta. \end{aligned} \tag{3.3}$$

with $\Omega=0.3$, $\lambda=0.4$ and $\mu=-1.5$. This figure illustrates both the true attractor and checkerboard approximations of it. The latter contain 50 and 10^3 curves obtained by laying down concentric circles, $r=c$, on the annulus. Since the curves now are not equally spaced in a rectilinear coordinate, the checkerboard squares are consequently not uniform. The attractor on the checkerboard interval looks like a plot of r against r', and modulo one square it resembles θ against θ'.

In the area-preserving limit, a special case of the annulus map is the Chirikov–Taylor (or standard) map,

$$\begin{aligned} \theta' &= \theta+r+\mu\sin\theta,\\ r' &= r+\mu\sin\theta. \end{aligned} \tag{3.4}$$

Although this map has a structure typical of a Hamiltonian map, and contains curves only in the form of nested periodic contours surrounded by unstructured chaotic regions, we can still use the checkerboarding method to approximate it. Then

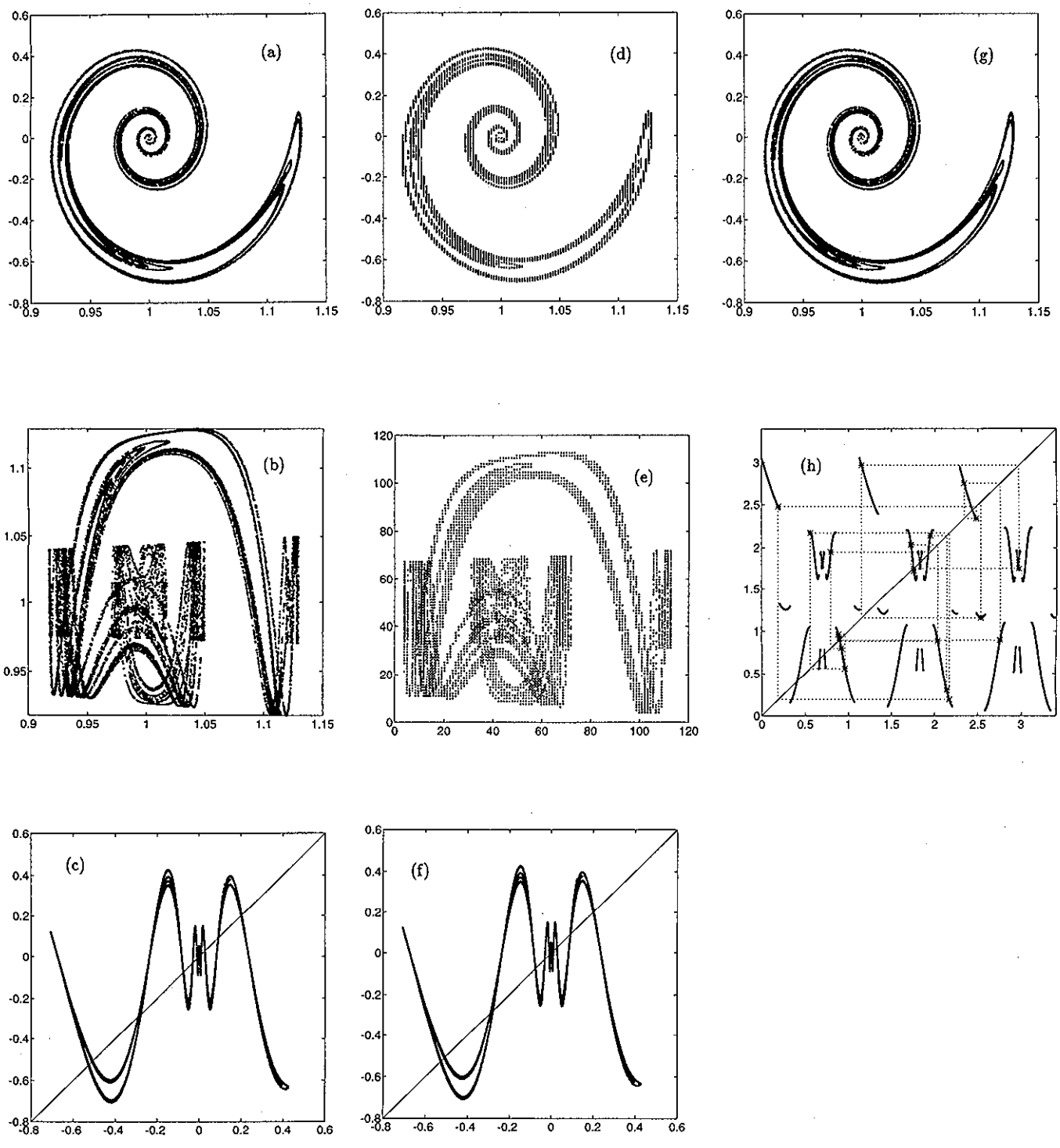

FIG. 8. Checkerboards of the Shil'nikov map, (3.2). Panels (a)–(c) show the actual attractor; plotted are x against z, then x against x', and finally z against z'. Panels (d)–(f) show an approximate attractor constructed using 100 curves. In (d), x is plotted against z. Panel (e) shows the attractor on the checkerboard (which increasingly resembles x against x'). Panel (f) shows the attractor modulo one square of the checkerboard (which approximates z against z'). Panel (g) shows an approximate attractor constructed with 1000 curves. Panel (h) shows the checkerboard map with $K=3$, plus a sample iteration.

we get the results displayed in Fig. 10. Lower-order approximations are not very successful in reproducing the features of the map, but higher-order ones do mimic the periodic island chains and chaotic seas.

IV. THE ANALYSIS

The tractability of dynamical systems diminishes rapidly as we go to high dimensions. We are suggesting a procedure

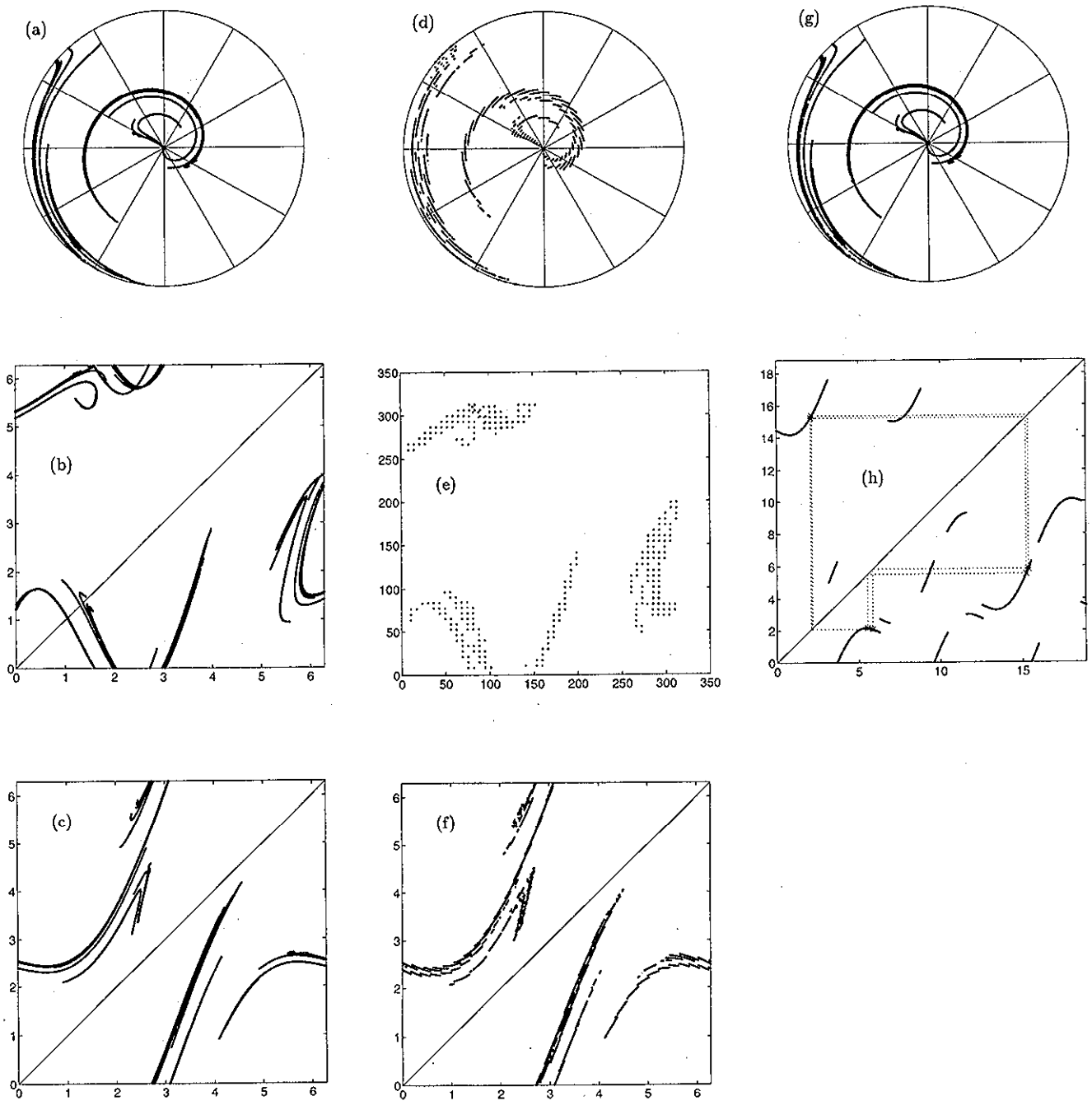

FIG. 9. Checkerboards of the annulus map, (3.3). Panels (a)–(c) show the actual attractor. (a) is a polar plot of (r,θ); (b) shows r against r'; panel (c) displays θ against θ'. In panels (d)–(f), the attractor of the checkerboard with 50 curves is portrayed. Panel (d) shows the (r,θ) polar plot; panel (e) shows the attractor on the checkerboard (which resembles a plot of r against r'); panel (f) shows the attractor, modulo one square of the checkerboard (which approximates θ against θ'). In panel (g), the checkerboard attractor is shown for $K=10^3$, and in (h), the checkerboard map with $K=3$ is displayed (together with a stable, period-6 orbit).

for redressing this loss, at least for n-dimensional maps with a single positive Lyapunov exponent. The example of the Hénon map, whose attractor is comprised of entwined, almost parabolic threads, provides a straightforward application of our methods. It also shows that, if we want to think of even the simplest higher dimensional maps in one-dimensional terms, we must accept the complications that numerous discontinuities introduce.

Above all, our procedure has conceptual advantages. For example, when many branches of the checkerboard approximation have critical points, it becomes immediately evident why the coexistence of many attractors in the map is generic and why the symbolic dynamics is extremely complicated. Though this may be known in some theoretical sense, it would be hard to make this fact appear more simply. Moreover, we may hope to facilitate the calculation of some mea-

(a) Standard map

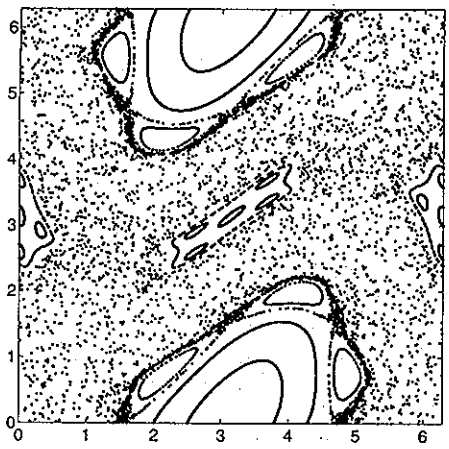

(b) 10^3−curve checkerboard

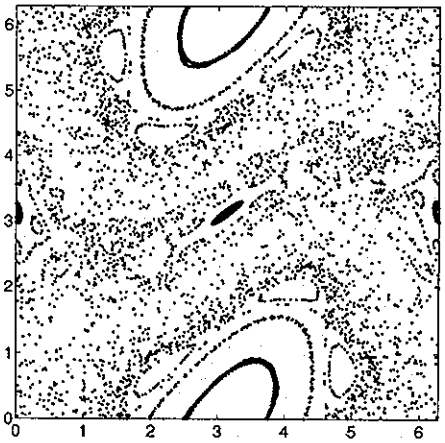

(c) 10^6−curve checkerboard

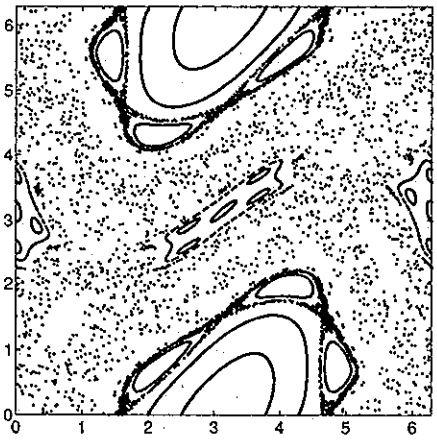

FIG. 10. The standard map, (3.4), and its checkerboard, with parameter value $\mu = 1.5$. Shown are successive mappings beginning from a variety of initial conditions on the (r, θ) plane. Panel (a) shows the exact map, panel (b) the checkerboard with 1000 curves, and panel (c) the checkerboard with 10^6 curves.

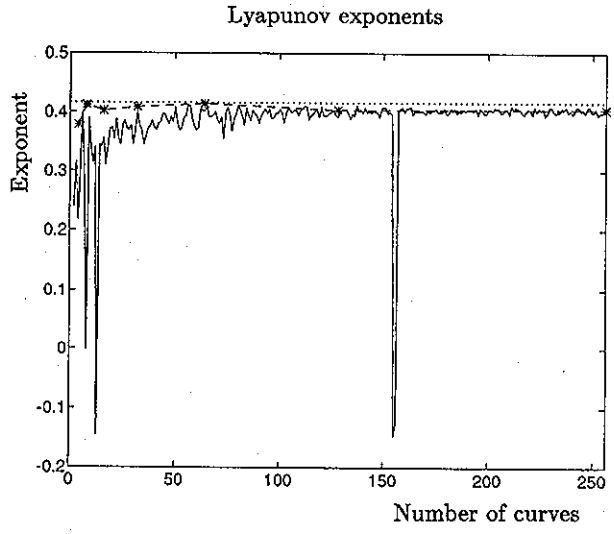

FIG. 11. Lyapunov exponents for the Hénon map and its checkerboard approximations ($a = 1/4$, $b = 0.3$). The horizontal dotted line shows the value of the expanding exponent of the true map. The dashed line and stars shows the exponent calculated using the asymptotic technique as a function of the number of curves. The solid line shows the same for the dynamically founded technique.

sures of complexity, such as topological entropy, with checkerboard maps. Although we do not know whether these measures for the checkerboard converge to the analogous measures for the original map as $K \to \infty$, we suggest that the values calculated from the checkerboards may themselves provide useful measures of complexity of the full system. We must mention that there are exceptions such as Lyapunov exponents, for which we can hope to get only the largest one. As we see from Fig. 11 even this may not be well approximated. Such discrepancies are not surprising because Lyapunov exponents are discontinuous functions of parameters.

In the final analysis, the reduction of higher dimensional maps to one dimension seems to be an effective way to visualize these complex objects. It is frequently supposed that maps in higher dimension are hard to think about simply because high dimensions are hard to visualize. Here we see that even when many of these maps can be dimensionally reduced, their dynamics does not immediately simplify. Yet, having made such a reduction, we may be in a position to think more productively about higher dimensional dynamics.

ACKNOWLEDGMENTS

In working at the problem dealt with here we have had the loyal assistance of our friend and colleague G. R. Ierley. We also had the benefit of financial support of the A.F.O.S.R. under Grant No. F49620-92-3-0061 at Columbia University.